Treatment-Related Uptake of *O*-(2-^{18}F-Fluoroethyl)-L-Tyrosine and L-[Methyl-^{3}H]-Methionine After Tumor Resection in Rat Glioma Models

Stefanie Geisler*[1], Carina Stegmayr*[1], Nicole Niemitz[1], Philipp Lohmann[1], Marion Rapp[2], Gabriele Stoffels[1], Antje Willuweit[1], Norbert Galldiks[1,3,4], Christian Filss[1,5], Michael C. Sabel[2], Heinz H. Coenen[1], Nadim Jon Shah[1,6,7], and Karl-Josef Langen[1,5,7]

[1]*Institute of Neuroscience and Medicine, Forschungszentrum Jülich, Jülich, Germany;* [2]*Department of Neurosurgery, Heinrich-Heine University, Düsseldorf, Germany;* [3]*Department of Neurology, University of Cologne, Cologne, Germany;* [4]*Center of Integrated Oncology, Universities of Bonn and Cologne, Cologne, Germany;* [5]*Department of Nuclear Medicine, RWTH Aachen University, Aachen, Germany;* [6]*Department of Neurology, RWTH Aachen University, Aachen, Germany; and* [7]*Section JARA–Brain, Jülich-Aachen Research Alliance, Aachen, Germany*

Assessment of residual tumor after resection of cerebral gliomas can be difficult with MRI and may be improved by amino acid PET. The aim of this experimental study was to investigate uptake of 2-^{18}F-fluoroethyl-L-tyrosine (^{18}F-FET) and L-[methyl-^{3}H]-methionine (^{3}H-MET) in residual tumor after surgery and possible false-positive uptake in treatment-related changes. **Methods:** F98 or GS-9L rat gliomas were implanted into the brain of 64 rats. Tumors were resected after 1 wk of tumor growth, and sham surgery was performed in an additional 10 animals. At different time points after surgery (1, 2, 3, 7, and 14–16 d), rats underwent ex vivo dual-tracer autoradiography using ^{18}F-FET and ^{3}H-MET. Histologic slices were evaluated by immunostaining for cell density and astrogliosis. Tracer uptake was quantified by lesion-to-brain ratios (L/B) at the rim of the resection cavity (considered treatment-related uptake) and in residual or recurrent tumor tissue. Four animals showing no residual tumor underwent PET 3 d after surgery to examine time–activity curves of ^{18}F-FET uptake in treatment-related changes. **Results:** Treatment-related uptake with a mean L/B of 2.0 ± 0.3 for ^{18}F-FET and a mean L/B of 1.7 ± 0.2 for ^{3}H-MET was noted at the rim of the resection cavity in the first week after surgery, decreasing significantly by 14–16 d ($P < 0.01$). Treatment-related tracer uptake was significantly higher for ^{18}F-FET than for ^{3}H-MET ($P < 0.001$). Tracer uptake in rat gliomas exceeded treatment-related tracer uptake at all time points ($P < 0.001$), but the latter was in the range of human gliomas. Reactive astrogliosis was noted near the resection cavity from the second day after surgery. Time–activity curves of ^{18}F-FET uptake in those areas revealed constantly increasing uptake. **Conclusion:** Surgery may induce significant treatment-related ^{18}F-FET and ^{3}H-MET uptake near the resection cavity in the first week after surgery, presumably caused by reactive astrogliosis. Treatment-related tracer uptake was less pronounced for ^{3}H-MET, indicating that ^{11}C-MET may be better suited for assessing the postoperative situation than ^{18}F-FET. Assessment of residual tumor after surgery by amino acid PET seems to be more reliable after an interval of 14 d.

Key Words: 2-^{18}F-fluoroethyl-L-tyrosine; ^{18}F-FET; L-[methyl-^{3}H]-methionine; ^{3}H-MET; glioma; PET; tumor resection

J Nucl Med 2019; 60:1373–1379
DOI: 10.2967/jnumed.119.225680

Next to meningiomas, gliomas are the most common primary brain tumors of the central nervous system with an incidence of 5–6 per 100,000 person-years (*1*). Despite intensive multimodal treatment strategies, most gliomas are associated with a poor prognosis (*2*).

Maximal cytoreductive surgery is a mainstay in the treatment of malignant gliomas and correlates with the efficacy of adjuvant treatment and prolonged survival (*3–8*). Therefore, a reliable identification and quantification of residual tumor after surgical resection are crucial to assess the success of tumor removal and patient outcome. Furthermore, a precise definition and localization of residual tumor mass are important for subsequent treatment planning such as early reoperation or radiation therapy.

MRI is currently the gold standard for the diagnostic evaluation of brain neoplasms because of its excellent soft-tissue contrast (*9*). Postoperative contrast-enhanced MRI is recommended within 72 h since later contrast-enhancing granulation tissue occurs at the margins of the resection cavity that cannot be distinguished from enhancing residual tumor parts (*10*). A lack of contrast enhancement, however, does not exclude residual tumor tissue, since a considerable part of malignant gliomas is nonenhancing and tumor tissue may extend beyond the area of contrast enhancement (*11*).

PET using radiolabeled amino acids such as 2-^{18}F-fluoroethyl-L-tyrosine (^{18}F-FET) and the long established L-[methyl-^{3}H]-methionine (^{11}C-MET) allows improved delineation of cerebral gliomas independent of contrast enhancement in MRI and has been recommended as an additional tool for brain tumor management (*12,13*).

The potential of amino acid PET to determine the extent of glioma resection has been addressed in several studies, which consistently reported a diagnostic gain compared with conventional MRI (*14–18*). The time frame of PET examinations after surgery, however, varies between studies, and so far no experimental study has investigated this aspect systematically. Both ^{18}F-FET and ^{11}C-MET have been

Received Jan. 2, 2019; revision accepted Feb. 20, 2019.
For correspondence or reprints contact: Karl-Josef Langen, Institute of Neuroscience and Medicine (INM-4), Forschungszentrum Jülich, D-52425 Jülich, Germany.
E-mail: k.j.langen@fz-juelich.de
*Contributed equally to this work.
Published online Mar. 8, 2019.

used to assess tumor resection in previous studies, though ^{18}F-FET is increasingly used in clinical practice because of the logistical advantages of the longer half-life of ^{18}F (*9,19*).

In an ongoing clinical PET study on tumor surgery, using ^{18}F-FET, new or increased tracer uptake near the tumor resection compared with the preoperative state, decreasing over time, was observed in a significant proportion of patients (*20*). This finding is not unexpected, since transient non–tumor-related accumulations of amino acid tracers have also been observed in other brain lesions such as ischemias or hematomas (*21,22*).

The aim of this experimental study was to investigate the time course and degree of treatment-related tracer uptake of ^{18}F-FET and ^{3}H-MET (equivalent to ^{11}C-MET) after brain tumor resection in 2 different rat glioma models (F98 and GS-9L) using dual-tracer autoradiography.

MATERIALS AND METHODS

Study Design

The cerebral uptake of ^{18}F-FET and ^{3}H-MET after tumor resection was examined in 2 different rat glioma models (F98 and GS-9L). For this purpose, tumor cells were implanted intracerebrally and the tumor mass was resected after 1 wk. At different time points after tumor resection (1, 2, 3, 7 or 14 d), animals were examined by ex vivo dual-tracer autoradiography using ^{18}F-FET and ^{3}H-MET. Six animals per time point and per tumor model were investigated. Additionally, 10 control animals (2 per time point at 1, 2, 3, 7, or 16 d) underwent resection of normal brain tissue without previous tumor implantation. The different timing of the animals being examined at 16 d instead of 14 d (Table 1) after surgery was due to logistical reasons and will be subsequently referred to as 2 wk.

Furthermore, rat brain sections were examined by histologic and immunofluorescence staining to evaluate the extent of tumor resection and reactive astrogliosis. The results were correlated with ^{18}F-FET and ^{3}H-MET accumulation gained by ex vivo autoradiography.

Four additional animals (F98 model) underwent ^{18}F-FET PET 3 d after tumor resection to gain information about the kinetic behavior of ^{18}F-FET in the area of resection.

Radiotracers

The amino acid *O*-(2-^{18}F-fluorethyl)-L-tyrosine (^{18}F-FET) was produced via nucleophilic ^{18}F-fluorination with a molar radioactivity of more than 18 TBq/mmol as described previously (*23*). ^{3}H-MET was obtained commercially with a molar activity of 3 GBq/mmol and a concentration of 37 MBq/mL (PerkinElmer).

Animal Experiments

Animal experiments were performed according to the German Law on the Protection of Animals (LANUV NRW Recklinghausen/Germany no. 84-02.04.2012.A447). The rats were housed under standard conditions with free access to food and water.

Male Fischer 344 rats (~220–350 g; Charles River Wiga Deutschland GmbH) were implanted with syngeneic F98 (n = 34) or GS-9L (n = 30) tumor cells. Stereotactic tumor implantation was performed as previously described with minor modifications (*24*). Briefly, according to a stereotactic brain atlas (*25*), 50,000 F98 or GS-9L cells (5 μL) were implanted intracerebrally (2 mm anterior and 3 mm lateral [left] to bregma; depth, 1.5 mm). The animals received a mixture of analgesics for 3 d after implantation (flunixin, 1 mg/kg of body weight; tramadol, 40 mg/kg of body weight).

Tumors were resected 7 d after implantation with the aim of total resection. For this purpose, animals were anesthetized with an intraperitoneal injection of a mixture of ketamine (100 mg/kg of body weight) and xylazine (10 mg/kg of body weight). The head was fixed in a stereotactic frame, and the skin of the skull was incised to expose the cranial bone. Around the borehole of the previous tumor

TABLE 1
Data on L/B and T/B of ^{18}F-FET and ^{3}H-MET Uptake After Resection of F98 or GS-9L Gliomas or Normal Brain Tissue

Animal model	Days after resection	L/B ^{18}F-FET	T/B mean ^{18}F-FET	L/B ^{3}H-MET	T/B mean ^{3}H-MET
F98	1	1.97 ± 0.20	4.19 ± 1.00	1.71 ± 0.17	6.88 ± 0.41
F98	2	1.74 ± 0.16	NA*	1.52 ± 0.12	NA*
F98	3	1.97 ± 0.11	4.77 ± 0.34	1.62 ± 0.16	5.91 ± 1.20
F98	7	2.00 ± 0.29	5.43 ± 0.39	1.53 ± 0.22	5.55 ± 0.63
F98	14	1.77 ± 0.10	4.85 ± 0.64	1.36 ± 0.08	4.66 ± 0.80
GS-9L	1	1.95 ± 0.16	4.40 ± 0.30	1.59 ± 0.11	7.36 ± 1.41
GS-9L	2	1.92 ± 0.24	4.24 ± 0.28	1.64 ± 0.20	5.77 ± 2.60
GS-9L	3	2.14 ± 0.16	4.43 ± 0.37	1.66 ± 0.16	7.06 ± 0.99
GS-9L	7	2.23 ± 0.22	4.89 ± 0.68	1.71 ± 0.16	6.41 ± 0.17
GS-9L	14	1.80 ± 0.20	4.62 ± 0.52	1.40 ± 0.09	5.84 ± 1.95
Control	1	2.54 ± 0.08	NA†	1.76 ± 0.08	NA†
Control	2	2.36 ± 0.30	NA†	2.05 ± 0.22	NA†
Control	3	1.99 ± 0.13	NA†	1.50 ± 0.19	NA†
Control	7	2.37 ± 0.17	NA†	1.81 ± 0.30	NA†
Control	16	1.38 ± 0.03	NA†	1.40 ± 0.01	NA†

*Residual tumor too small for evaluation.
†Control animals without tumor implantation.
NA = not available.

implantation, a cranial bone fragment (~5 × 7 mm) was removed using a microdrill and tweezers. The tumor was totally resected using microsurgical scissors as far as visually recognizable. After resection, the cranial window was covered with hemostatic gauze to support hemostasis and the incision was sutured. The animals received analgesics as described above. Resection of normal brain tissue (control animals) was performed in an analogous manner.

Dual-Tracer Autoradiography

At different time points after tumor resection (1, 2, 3, or 7 d or 2 wk), animals were sedated in a 2%–5% atmosphere of isoflurane. A mixture of the radiotracers ^{18}F-FET (~70 MBq) and ^{3}H-MET (~11 MBq) was injected into the tail vein. The rats were killed 60 min after injection by decapitation, and the brains were removed, frozen, cut in coronal sections (20 μm) and placed on photo imager plates as described previously (*24*). ^{18}F-FET and ^{3}H-MET autoradiograms were generated and coregistered to parallel histologic slices by drawing a circumference region of interest (ROI) along the borders of the 4′,6-diamidino-2-phenylindole dihydrochloride (DAPI)–stained histologic slices (see below) and adapting the size of the corresponding autoradiogram to that ROI. Autoradiograms and histologic slices were compared visually by 3 experienced scientists in consensus. The autoradiograms were semiquantitatively evaluated by ROIs using commercial software (AIDA, version 4.50; raytest Isotopenmessgeräte GmbH). Circular ROIs (size, 1.3–1.5 mm^2) were placed on tumor-free areas with a maximum of abnormal ^{18}F-FET uptake at the rim of the resection cavity (considered treatment-related uptake) and in areas of maximum tracer uptake in residual or recurrent tumor (ROI size, 0.7–1.5 mm^2). A larger reference ROI was placed in the contralateral hemisphere in unaffected brain tissue (ROI size, 3.4–3.5 mm^2). These ROIs were transferred to the corresponding ^{3}H-MET autoradiograms to ensure identical evaluation for both tracers. Maximum lesion-to-brain ratio (L/B) or tumor-to-brain ratio (T/B) was calculated by dividing tracer uptake in these ROIs by tracer uptake in the normal brain.

Small-Animal ^{18}F-FET PET

Dynamic PET studies were acquired 3 d after resection of F98 gliomas in 4 animals under isoflurane anesthesia (1.5%–2.0%) up to 61 min after intravenous injection of approximately 35 MBq of ^{18}F-FET on an Inveon Scanner (Siemens Preclinical Solutions, Inc.) in 3-dimensional mode (1.51 × 1.51 × 10 mm lutetium oxyorthosilicate crystal elements; 16.1-cm ring diameter; 10-cm transaxial field of view; 12.7-cm axial field of view). The emission data consisted of 26 time frames (6 × 10 s, 5 × 60 s, 5 × 180 s, 10 × 240 s). Data were corrected for scattered coincidences, attenuation, decay, and dead time and reconstructed using filtered backprojection, resulting in voxel sizes of 0.7764 × 0.7764 × 0.796 mm. ^{18}F-FET uptake in the tissue was expressed as SUV by dividing the radioactivity in the tissue by the injected tracer dose per gram of body weight (PMOD, version 3.4; PMOD Technologies Ltd.). The volumes of interest were analyzed in averaged time frames of 18–61 min after tracer injection. ^{18}F-FET uptake in the unaffected brain tissue was determined by a volume of interest (120 mm^3) placed on the contralateral hemisphere in an area of unaffected striatal brain tissue. Uptake in the area of resection was determined by a 3-dimensional auto-contouring process using a threshold of 1.4 above contralateral uptake. Time–activity curves were generated from SUV_{mean} in the resection area and in the unaffected brain. After PET acquisition, the animals were killed and cryosections of the brains were produced for histologic staining to confirm total resection of tumor.

^{18}F-FET PET in rats was performed 3 d after surgery, as the histologic data show minimal tumor recurrence at this time point and thus optimal tumor-free tracer uptake.

Fluorescence Staining

Reactive astrocytes were detected by immunofluorescence staining for glial fibrillary acidic protein (GFAP) using a rabbit antirat GFAP polyclonal antibody (1:1,000; Abcam). As a secondary fluorochrome-conjugated antibody, goat-antirabbit Alexa Fluor 488 (1:300; Invitrogen) was used. In all slices, cell nuclei were counterstained with DAPI for histologic analysis of cell density.

Statistical Analysis

Each value of L/B or T/B is expressed as the mean ± SD. Four to 6 brain sections of each tumor animal were analyzed to calculate the mean L/B, and 2 brain sections were analyzed for T/B. In control animals, 3 sections of each animal were used to determine the respective L/B. ROIs for ^{18}F-FET and ^{3}H-MET were congruent. Animals with a minimal residual tumor extent (too small for ROI placement) were not included in determination of T/Bs. A Pearson correlation and a 3-way ANOVA with the factors "time after resection" (1, 2, 3, and 7 d; 2 wk), "model" (control, F98, 9L) and "tracer" (^{18}F-FET, ^{3}H-MET) were applied to assess differences in L/B with respect to the 3 factors using the SigmaPlot software (version 12.5; Systat Software Inc.). *P* values of less than 0.05 were considered to be statistically significant.

RESULTS

Treatment-Related Tracer Uptake After Surgical Intervention

The mean values of L/B and T/B at different time points after tumor resection in the 2 tumor models and on brain resection in control animals are given in Table 1. In both tumor models and control animals, a diffuse but distinct treatment-related uptake was noticed near the resection cavity within the first 7 d after resection, with a mean L/B of 2.0 ± 0.3 for ^{18}F-FET and a mean L/B of 1.7 ± 0.2 for ^{3}H-MET. A representative example of a 9L glioma 2 d after surgery is shown in Figure 1.

Overall, relevant residual or recurrent tumor tissue as identified by DAPI staining on the histologic slices was present in 58% of the animals, but this percentage varied depending on the interval after surgery. Within the first 3 d after surgery, 61% of the animals showed no or only minimal residual tumor, whereas after an interval of 7 d or more the resection cavities were partially or completely overgrown by recurrent tumor in 88% of the animals (data not shown).

Immunofluorescence staining against GFAP revealed reactive astrocytes near the resection cavity, as well as residual tumors, from the second day after surgery, which partly matched with treatment-related ^{18}F-FET and ^{3}H-MET uptake in autoradiograms (Fig. 1).

The time course of treatment-related ^{18}F-FET and ^{3}H-MET uptake at different time points after normal brain tissue resection is further illustrated in Figure 2. The figure demonstrates the results of 5 control animals to exclude an influence of residual tumor. There is prominent treatment-related tracer accumulation within the first 7 d after resection, especially for ^{18}F-FET, decreasing to low values at 2 wk after resection.

The quantified time course of treatment-related ^{18}F-FET and ^{3}H-MET uptake after brain surgery for both tumor models and control animals is shown in Figure 3. There is increased tracer uptake at the rim of the resection cavity for both tracers, decreasing significantly at 2 wk after resection ($P \leq 0.01$). ^{3}H-MET uptake near the resection cavity was significantly lower than ^{18}F-FET uptake at each time point ($P < 0.001$).

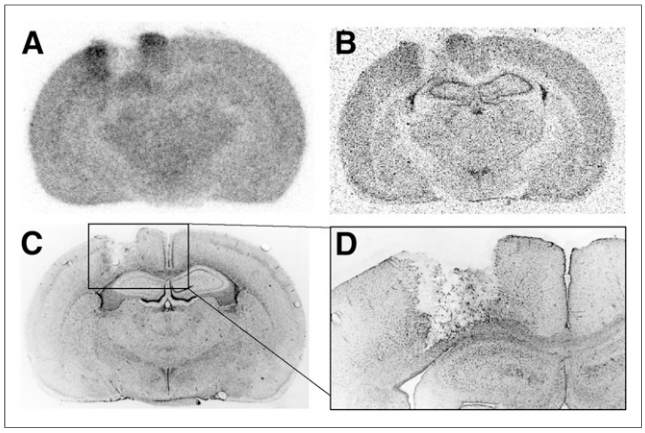

FIGURE 1. Coronal rat brain sections 2 d after resection of 9L glioma: ^{18}F-FET (A) and ^{3}H-MET (B) autoradiography, DAPI immunofluorescence staining (C), and magnified view of GFAP staining at rim of resection cavity (D). There is increased tracer uptake at rim of resection cavity and reactive astrocytosis.

L/Bs of F98 and GS-9L differed significantly ($P < 0.05$) with respect to the different tracers on days 2 and 7 after resection, whereas the control animals differed ($P < 0.01$) from both tumor models on days 1 and 2 after resection. Besides other differences between the 3 models in L/Bs over the period of 14 d, in both tumor models the treatment-related ^{18}F-FET and ^{3}H-MET uptake decreased significantly ($P < 0.05$) from day 3 and 7 to 2 wk after resection (Fig. 3). In the control group, treatment-related uptake of both tracers was lowest at 2 wk but highest was on days 1 and 2 (Fig. 3; Table 1).

L/Bs of both tracers differed significantly from each other ($P < 0.001$) but positively correlated with each other ($P < 0.0001$, $r = 0.67$), with higher L/Bs in ^{18}F-FET (Fig. 4).

On each day after surgery, treatment-related ^{18}F-FET and ^{3}H-MET uptake was significantly lower near the resection area than in F98 or GS-9L tumors ($P < 0.001$, Table 1), so that tumor tissue could be differentiated from treatment-related tracer uptake in both tumor models.

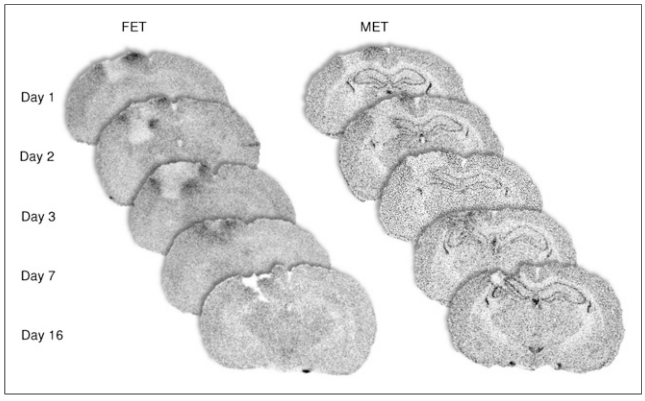

FIGURE 2. Autoradiographic brain slices of 5 different control animals at different time points after resection of normal brain tissue demonstrating time course of treatment-related ^{18}F-FET and ^{3}H-MET uptake near resection cavity. There is prominent treatment-related tracer accumulation within first 7 d after resection, especially for ^{18}F-FET, which decreases to low level 16 d after resection.

Dynamic ^{18}F-FET PET

Figure 5 shows an example of ^{18}F-FET PET 3 d after complete resection of a F98 rat glioma, demonstrating treatment-related ^{18}F-FET uptake in the resection area. The time–activity curves of ^{18}F-FET uptake in the resection area and in normal brain tissue of 4 animals 3 d after resection of F98 gliomas showed a constantly increasing ^{18}F-FET uptake with a significantly higher SUV in the area of resection than in normal brain tissue ($P < 0.001$). Histologic staining of rat brain sections after PET acquisition confirmed no solid residual tumor tissue (data not shown).

DISCUSSION

A precise evaluation of the extent of tumor resection is of great importance in the prognosis and treatment strategy for cerebral gliomas, which are routinely assessed only by conventional MRI, with limited reliability, as outlined above. Some clinical reports suggest that PET using radiolabeled amino acids can be helpful in this matter. Pirotte et al. reported that PET using ^{11}C-MET successfully detected residual tumor in 13 of 19 pediatric brain tumors, which were confirmed by repeated surgery or tumor progress in all cases (*16*). The same group reported on the prognostic role of residual tumor tissue by ^{11}C-MET PET in a group of 43 adults with high-grade glioma. Total tumor resection according to ^{11}C-MET PET correlated significantly with survival, whereas a total removal of contrast enhancement on MRI did not (*17*). In that study, ^{11}C-MET PET scans were performed in two thirds of patients within 8 d after surgery and in one third later than 6 wk without a clear rationale for this procedure. Using ^{18}F-FET PET, 2 studies with an overlapping patient population have so far addressed the problem of brain tumor resection (*14,15*). In those studies, residual tumor tissue was observed more frequently with ^{18}F-FET PET than with MRI. However, the actual presence of tumor tissue was confirmed histologically or by the further clinical course in a few cases only, thus limiting the informative value of the results from those studies. Furthermore, it was reported that the timing of ^{18}F-FET PET (<72 h vs. >72 h) had no influence on PET imaging results, or only early timing (72 h) was available. Considering that the presence of residual tumor tissue was not evaluated in that patient population, the influence of timing of amino acid PET in assessing residual tumor after surgery still remains unclear.

The results of the present study indicate that surgical resection of brain tumors may cause increased treatment-related uptake of ^{18}F-FET and ^{3}H-MET at the level of human gliomas (*26,27*) within the first week after resection and could therefore be misinterpreted as residual tumor. Treatment-related uptake of both examined tracers after surgery showed a significant correlation, but ^{3}H-MET uptake was less pronounced than ^{18}F-FET uptake, as is in line with previous results (*17*). This suggests that ^{11}C-MET may be better suited for assessing the postoperative situation than ^{18}F-FET. Nevertheless, because the uptake of both tracers is significantly increased within the first week after resection, the determination of residual tumor by amino acid PET seems to be more reliable after an interval of 14 d.

The temporal pattern of treatment-related increased ^{18}F-FET uptake after surgical injury is similar to observations in experimental ischemic lesions in the rat brain, which also decreased significantly after 14 d (*22*). In ischemic lesions, the areas of abnormal ^{18}F-FET uptake were largely congruent with areas of reactive astrogliosis, whereas in the present study GFAP staining

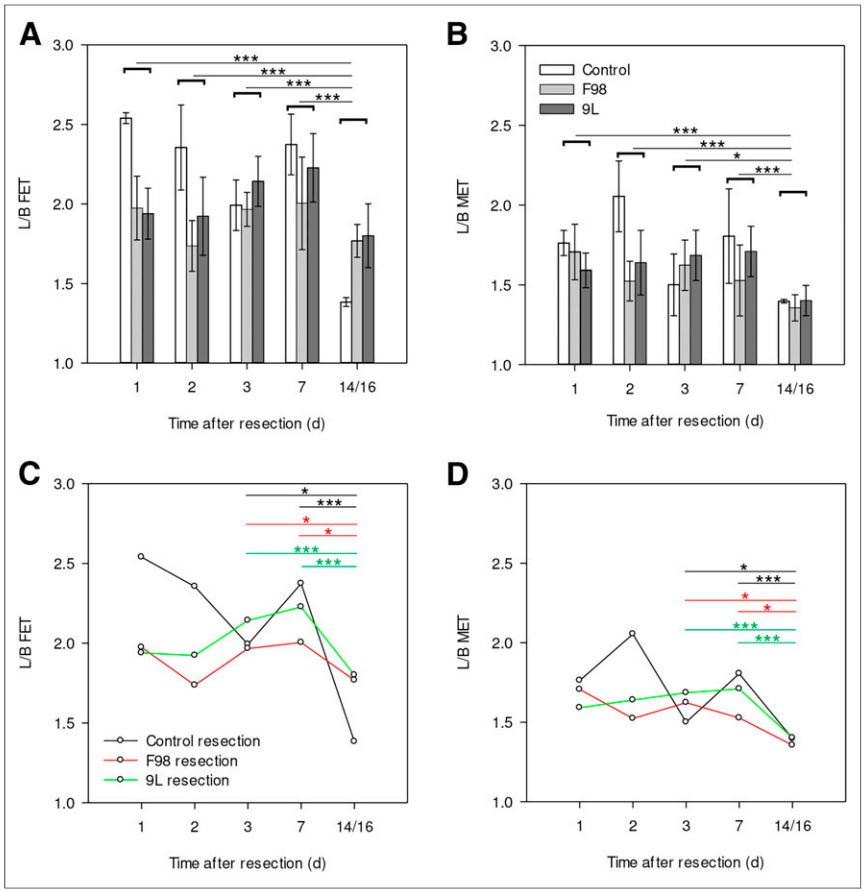

FIGURE 3. (A and B) Mean ± SD of L/B of treatment-related ^{18}F-FET (A) and ^{3}H-MET (B) uptake after resection of F98 gliomas, GS-9L tumors, and control animals. A and B show statistical difference between different time points after resection when using average value of all subgroups. Tracer uptake at rim of resection cavity decreases for both tracers on 14/16 d after resection. (C and D) Time course and statistical difference between individual subgroups (limited to comparison of day 3 or day 7 vs. 14/16 d after resection), which demonstrates that effect is present for all subgroups. $^{*}P \leq 0.05$. $^{**}P \leq 0.01$. $^{***}P \leq 0.001$.

only partly matched abnormal ^{18}F-FET uptake. Discrepancies between nonneoplastic ^{18}F-FET uptake and reactive astrogliosis have already been observed in experimental hematomas and near irradiated F98 gliomas (*21,28*). These discrepancies can be explained by the fact that reactive astrogliosis does not represent an all-or-nothing phenomenon but a complex process regulated in a context-dependent manner underlying molecular, cellular, and functional changes in response to all forms and severities of central nervous system injury (*29,30*). It seems that treatment-related uptake of ^{18}F-FET correlates with the presence of reactive astrogliosis only under specific conditions possibly depending on the physiologic state of astrocytes and their expression of large amino acid transporters. In addition to astrogliosis, other mechanisms for increased amino acid accumulation such as disruption of the blood–brain barrier, increased perfusion, or edema must also be discussed. In different preclinical and clinical studies (*31–35*), however, no significant influence of blood–brain barrier disruption, microvessel density, perfusion, or edema on ^{18}F-FET uptake has been reported. Furthermore, ^{18}F-FET is not involved in protein synthesis, but for ^{3}H-MET uptake, an influence of protein incorporation cannot be excluded. In previous studies with experimental infarcts and abscesses, an increased ^{3}H-MET accumulation was observed in areas with macrophage infiltration where ^{18}F-FET was negative (*22,36*). This pattern, however, was never observed in the current study, which virtually excludes a significant role of ^{3}H-MET accumulation due to increased protein synthesis in macrophages.

Another aspect investigated in this study is the kinetic pattern of ^{18}F-FET uptake in treatment-related changes after surgery. Time–activity curves of abnormal ^{18}F-FET uptake after total resection of F98 gliomas showed a constantly increasing uptake curve, which is typical for benign lesions. It is tempting to speculate that this feature could contribute to a distinction between postsurgical changes and tumor residuals of high-grade gliomas in humans as observed for other treatment-related changes in the further follow-up of gliomas (*37–39*). However, kinetic analysis would not be helpful in distinguishing between residuals of low-grade glioma and treatment-induced changes.

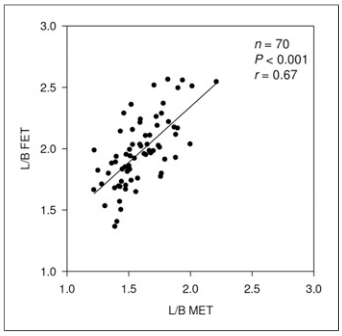

FIGURE 4. Comparison of L/B of ^{18}F-FET and ^{3}H-MET uptake at rim of resection cavity shows significant positive correlation. Regression line is shifted to left in relation to bisection line, demonstrating that L/B of treatment-related tracer accumulation is higher for ^{18}F-FET than for ^{3}H-MET.

This study had some limitations. It has to be considered that the results of animal experiments may not be transferable to the human situation for several reasons. First, only high-grade tumors are available in the rat model, so that the results may not be representative of the resection of low-grade gliomas in humans. Brain tissue resection in control animals without tumors, however, yielded similar results, indicating that the tissue responses do not differ significantly in the resection of high- and low-grade gliomas. Second, because the tissue reactions in rodents may be faster and more pronounced than in humans, the results need to be considered with caution. On the basis of preliminary observations in humans (*20*), however, similar phenomena appear to be present in humans and further clinical studies are urgently needed before amino acid PET can be used as a clinical tool to assess brain tumor resection. Third, the spatial resolution of the ^{3}H-MET autoradiograms is significantly higher than that of the ^{18}F-FET autoradiograms, and it cannot be ruled out that the L/Bs of ^{3}H-MET uptake are overestimated compared with ^{18}F-FET. Since tracer uptake was measured in identical ROIs with a relatively large size compared with the spatial resolution, this effect is likely to be of little importance. Finally, the autoradiographic data were measured 1 h after tracer injection whereas

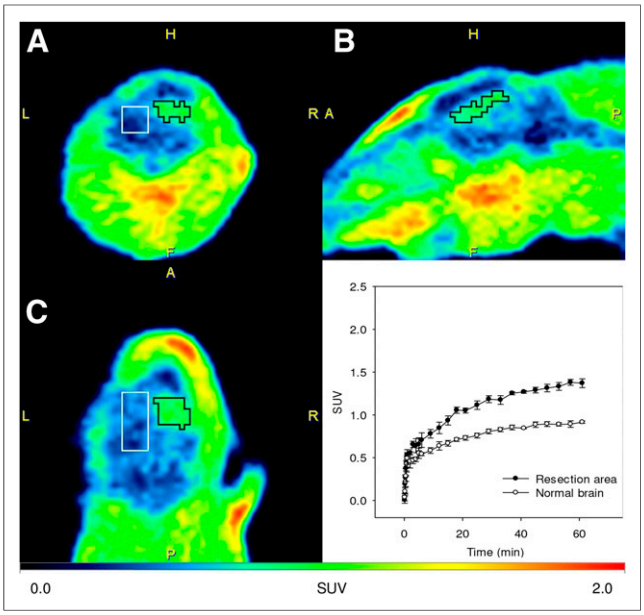

FIGURE 5. Examples of coronal (A), sagittal (B), and transversal (C) PET scans (18–61 min after injection) 3 d after resection of F98 rat glioma showing treatment-related ^{18}F-FET uptake near resection area. Histology indicated no residual tumor tissue. Time–activity curves (SUV ± SD, n = 4) show treatment-related ^{18}F-FET uptake in resection area compared with normal brain tissue of rats. Kinetic pattern shows constantly increasing ^{18}F-FET uptake in both regions.

PET examinations in humans are performed earlier, that is, 20–40 min after injection for ^{18}F-FET and 10–30 min after injection for ^{11}C-MET. Especially for ^{18}F-FET, the blood pool is relatively high in the first 30 min after injection, which could influence the results in terms of even more pronounced treatment-related changes.

CONCLUSION

The results of this experimental study demonstrate that surgical resection of brain tumors may induce treatment-related ^{18}F-FET and ^{3}H-MET uptake in the first week after surgery, presumably caused by reactive astrogliosis. Tracer uptake is on the order of magnitude of human gliomas and therefore could be misinterpreted as residual tumor. This treatment-related tracer uptake was less pronounced for ^{3}H-MET, indicating that ^{11}C-MET may be better suited for assessing the postoperative situation than ^{18}F-FET. Assessment of residual tumor after surgery by amino acid PET seems to be more reliable after an interval of 14 d.

DISCLOSURE

No potential conflict of interest relevant to this article was reported.

ACKNOWLEDGMENTS

We thank Daniela Schumacher for excellent technical assistance and Silke Grafmüller, Bettina Palm, Erika Wabbals, and Sascha Rehbein for radiosynthesis of ^{18}F-FET.

KEY POINTS

QUESTION: Does surgical removal of brain tumors cause a treatment-related accumulation of ^{18}F-FET and ^{3}H-MET?

PERTINENT FINDINGS: ^{18}F-FET and ^{3}H-MET uptake was evaluated by dual-tracer autoradiography at different time points after resection of intracerebral rat gliomas. Treatment-related uptake with a mean L/B of 2.0 ± 0.3 for ^{18}F-FET and a mean L/B of 1.7 ± 0.2 for ^{3}H-MET was noted at the rim of the resection cavity in the first week after surgery, which decreased significantly by 14–16 d.

IMPLICATIONS FOR PATIENT CARE: Assessment of residual tumor after surgery by amino acid PET seems to be more reliable after an interval of 14 d.

REFERENCES

1. Ostrom QT, Gittleman H, Liao P, et al. CBTRUS statistical report: primary brain and central nervous system tumors diagnosed in the United States in 2007-2011. *Neuro Oncol.* 2014;16(suppl 4):iv1–iv63.
2. Ohgaki H, Kleihues P. Population-based studies on incidence, survival rates, and genetic alterations in astrocytic and oligodendroglial gliomas. *J Neuropathol Exp Neurol.* 2005;64:479–489.
3. Stummer W, Reulen HJ, Meinel T, et al. Extent of resection and survival in glioblastoma multiforme: identification of and adjustment for bias. *Neurosurgery.* 2008;62:564–576.
4. Kuhnt D, Becker A, Ganslandt O, Bauer M, Buchfelder M, Nimsky C. Correlation of the extent of tumor volume resection and patient survival in surgery of glioblastoma multiforme with high-field intraoperative MRI guidance. *Neuro Oncol.* 2011;13:1339–1348.
5. Oszvald A, Guresir E, Setzer M, et al. Glioblastoma therapy in the elderly and the importance of the extent of resection regardless of age. *J Neurosurg.* 2012;116:357–364.
6. Sanai N, Polley MY, McDermott MW, Parsa AT, Berger MS. An extent of resection threshold for newly diagnosed glioblastomas. *J Neurosurg.* 2011;115:3–8.
7. McGirt MJ, Chaichana KL, Attenello FJ, et al. Extent of surgical resection is independently associated with survival in patients with hemispheric infiltrating low-grade gliomas. *Neurosurgery.* 2008;63:700–707.
8. Van den Bent M, Stupp R, Mason W, Mirimanoff R, Lacombe D, Gorlia T. Impact of extent of resection on overall survival in newly-diagnosed glioblastoma after chemo-irradiation with temozolomide: further analysis of EORTC study 26981. *Eur J Cancer Suppl.* 2005;3:134.
9. Langen KJ, Galldiks N, Hattingen E, Shah NJ. Advances in neuro-oncology imaging. *Nat Rev Neurol.* 2017;13:279–289.
10. Forsting M, Albert FK, Kunze S, Adams HP, Zenner D, Sartor K. Extirpation of glioblastomas: MR and CT follow-up of residual tumor and regrowth patterns. *AJNR Am J Neuroradiol.* 1993;14:77–87.
11. Scott JN, Brasher PM, Sevick RJ, Rewcastle NB, Forsyth PA. How often are nonenhancing supratentorial gliomas malignant? A population study. *Neurology.* 2002;59:947–949.
12. Albert NL, Weller M, Suchorska B, et al. Response Assessment in Neuro-Oncology Working Group and European Association for Neuro-Oncology recommendations for the clinical use of PET imaging in gliomas. *Neuro Oncol.* 2016;18:1199–1208.
13. Galldiks N, Dunkl V, Kracht LW, et al. Volumetry of [^{11}C]-methionine positron emission tomographic uptake as a prognostic marker before treatment of patients with malignant glioma. *Mol Imaging.* 2012;11:516–527.
14. Buchmann N, Klasner B, Gempt J, et al. F-18-fluoroethyl-L-tyrosine positron emission tomography to delineate tumor residuals after glioblastoma resection: a comparison with standard postoperative magnetic resonance imaging. *World Neurosurg.* 2016;89:420–426.
15. Kläsner B, Buchmann N, Gempt J, Ringel F, Lapa C, Krause BJ. Early [^{18}F]FET-PET in gliomas after surgical resection: comparison with MRI and histopathology. *PLoS One.* 2015;10:e0141153.
16. Pirotte B, Levivier M, Morelli D, et al. Positron emission tomography for the early postsurgical evaluation of pediatric brain tumors. *Childs Nerv Syst.* 2005;21:294–300.
17. Pirotte BJ, Levivier M, Goldman S, et al. Positron emission tomography-guided volumetric resection of supratentorial high-grade gliomas: a survival analysis in 66 consecutive patients. *Neurosurgery.* 2009;64:471–481.

18. Pirotte BJ, Lubansu A, Massager N, et al. Clinical impact of integrating positron emission tomography during surgery in 85 children with brain tumors. *J Neurosurg Pediatr.* 2010;5:486–499.
19. Langen KJ, Stoffels G, Filss C, et al. Imaging of amino acid transport in brain tumours: positron emission tomography with O-(2-[^{18}F]fluoroethyl)-L-tyrosine (FET). *Methods.* 2017;130:124–134.
20. Filss CP, Schmitz A, Stoffels G, et al. Increased FET-uptake after tumor resection in glioma patients [abstract]. *Nucl Med (Stuttg).* 2018;56(suppl):66.
21. Salber D, Stoffels G, Oros-Peusquens AM, et al. Comparison of O-(2-^{18}F-fluoroethyl)-L-tyrosine and L-^{3}H-methionine uptake in cerebral hematomas. *J Nucl Med.* 2010;51:790–797.
22. Salber D, Stoffels G, Pauleit D, et al. Differential uptake of [^{18}F]FET and [^{3}H]l-methionine in focal cortical ischemia. *Nucl Med Biol.* 2006;33:1029–1035.
23. Hamacher K, Coenen HH. Efficient routine production of the ^{18}F-labelled amino acid O-2-^{18}F fluoroethyl-L-tyrosine. *Appl Radiat Isot.* 2002;57:853–856.
24. Geisler S, Willuweit A, Schroeter M, et al. Detection of remote neuronal reactions in the thalamus and hippocampus induced by rat glioma using the PET tracer cis-4-[^{18}F]fluoro-D-proline. *J Cereb Blood Flow Metab.* 2013;33:724–731.
25. Paxinos G, Watson C. *The Rat Brain in Stereotaxic Coordinates: The New Coronal Set.* 5th ed. Cambridge, MA: Academic Press; 2004.
26. Rapp M, Heinzel A, Galldiks N, et al. Diagnostic performance of ^{18}F-FET PET in newly diagnosed cerebral lesions suggestive of glioma. *J Nucl Med.* 2013;54:229–235.
27. Herholz K, Holzer T, Bauer B, et al. ^{11}C-methionine PET for differential diagnosis of low-grade gliomas. *Neurology.* 1998;50:1316–1322.
28. Piroth MD, Prasath J, Willuweit A, et al. Uptake of O-(2-[^{18}F]fluoroethyl)-L-tyrosine in reactive astrocytosis in the vicinity of cerebral gliomas. *Nucl Med Biol.* 2013;40:795–800.
29. Sofroniew MV, Vinters HV. Astrocytes: biology and pathology. *Acta Neuropathol (Berl).* 2010;119:7–35.
30. Sofroniew MV. Molecular dissection of reactive astrogliosis and glial scar formation. *Trends Neurosci.* 2009;32:638–647.
31. Spaeth N, Wyss MT, Pahnke J, et al. Uptake of ^{18}F-fluorocholine, ^{18}F-fluoroethyl-L-tyrosine and ^{18}F-fluoro-2-deoxyglucose in F98 gliomas in the rat. *Eur J Nucl Med Mol Imaging.* 2006;33:673–682.
32. Stegmayr C, Bandelow U, Oliveira D, et al. Influence of blood-brain barrier permeability on O-(2-^{18}F-fluoroethyl)-L-tyrosine uptake in rat gliomas. *Eur J Nucl Med Mol Imaging.* 2017;44:408–416.
33. Stegmayr C, Oliveira D, Niemietz N, et al. Influence of bevacizumab on blood-brain barrier permeability and O-(2-^{18}F-fluoroethyl)-l-tyrosine uptake in rat gliomas. *J Nucl Med.* 2017;58:700–705.
34. Filss CP, Galldiks N, Stoffels G, et al. Comparison of ^{18}F-FET PET and perfusion-weighted MR imaging: a PET/MR imaging hybrid study in patients with brain tumors. *J Nucl Med.* 2014;55:540–545.
35. Lohmann P, Stavrinou P, Lipke K, et al. FET PET reveals considerable spatial differences in tumour burden compared to conventional MRI in newly diagnosed glioblastoma. *Eur J Nucl Med Mol Imaging.* 2019;46:591–602.
36. Salber D, Stoffels G, Pauleit D, et al. Differential uptake of O-(2-^{18}F-fluoroethyl)-L-tyrosine, L-^{3}H-methionine, and ^{3}H-deoxyglucose in brain abscesses. *J Nucl Med.* 2007;48:2056–2062.
37. Weckesser M, Langen KJ, Rickert CH, et al. O-(2-[^{18}F]fluorethyl)-L-tyrosine PET in the clinical evaluation of primary brain tumours. *Eur J Nucl Med Mol Imaging.* 2005;32:422–429.
38. Galldiks N, Dunkl V, Stoffels G, et al. Diagnosis of pseudoprogression in patients with glioblastoma using O-(2-[^{18}F]fluoroethyl)-L-tyrosine PET. *Eur J Nucl Med Mol Imaging.* 2015;42:685–695.
39. Galldiks N, Stoffels G, Filss C, et al. The use of dynamic O-(2-^{18}F-fluoroethyl)-l-tyrosine PET in the diagnosis of patients with progressive and recurrent glioma. *Neuro Oncol.* 2015;17:1293–1300.